 CMES, vol.94, no.3, pp.261-277, 2013

Numerical Simulation of 2-D Transversal Seismic Waves by Network Method

J.L. Morales[1], I. Alhama[1], M. Alcaraz[1] and F. Alhama

Abstract: In this paper, the propagation of 2-D, transversal elastic waves is simulated by using the network method. The spatially discretized wave equation is the basis for designing the model of the volume element which contains as many components as addends in the governing equation. The whole network model, including the boundary conditions, is run in a suitable circuit simulation code such as PSpice with a relatively small computational time. The rules for the design are very few since there is a special component in the libraries of such codes, named controlled source, that is capable of implementing any kind of non-linearity or coupled term in the equation. The design routines as well as those required for the subsequent post-processing of output data are carried out by MATLAB. After the study and simulation of a standard case, in order to compare the network solutions with those obtained by the finite-difference explicit method, two problems are presented using the known Ricker pulse as excitation.

Keywords: SH seismic waves, Numerical simulation, Network simulation method.

1 Introduction

The network method is a numerical tool, which has been extensively used in recent years for successfully solving a large variety of problems in science and engineering [Morales et al. (2011); Moreno et sal. (2007); Soto et al. (2007)]. In this paper the technique is applied for the first time to solve 1-D and 2-D transversal (SH) seismic waves problems, a scenarios already investigated by other numerical methods [Simos and Vigo-Aguilar (2003), Natesan et al. (2003), Martin-Vaquero and Vigo-Aguilar (2006) and Vigo-Aguilar and Natesan (2006), Akbarti et al. (2010), Zhuang et al. (2011,2012].

Despite the disadvantage of the need to be familiar with the basic principles of electric circuit theory, the proposed method [González Fernández (2002)] has demonstrated itself to be an accurate and reliable tool for many researchers. Although it

[1] Universidad Politécnica de Cartagena (UPCT), Spain.

is based on the electric analogy widely treated in many books, particularly in heat transfer problems for educational purposes [Mills (1995); Incropera and De Witt (1996)], when it serves –as an alternative representation of a problem in the context of the general analogy between equations–, it goes far beyond the scope of this subject and can be used as a real numerical tool, making good use of the powerful algorithms implemented in the circuit simulation codes. In addition, no mathematical manipulations are required to treat the finite-difference equations that normaly have to be solved by iteration; this work is done by the code. In this context and for the first time, we apply the method to obtain the solution of the wave equation: the emergence and propagation of transversal elastic waves in 1-D and 2-D domains from the point source.

The starting point for the design of the model is the finite-difference differential equation that results from the spatial discretization of the mathematical model. The addends of this equation are assumed to be electrical currents that are balanced, according to their signs, at a common node of the network, the voltage of which is generally the solution to the equation. The implementation of each addend in the network is made by choosing an electrical component or device whose equation is simply that of the addend obtained by substituting the dependent variables of the physical processes by their analogous ones (electric current and voltage). Most of the linear terms of the PDEs are easily implemented in the model by simple devices (resistors, capacitors and coils), while non-linear or coupled addends require special devices named controlled current sources, as defined in the libraries of the electric simulation codes, that make the implementation of these non-linear or coupled terms a straightforward task. In addition, second order time derivative or other possible derivative terms of a higher order require auxiliary networks to be designed. These controlled sources, whose output current can be specified by software as a function of other variables defined at any point (voltage) or any component (current) of the model, in combination with auxiliary circuits if required, allow any mathematical problem to be designed regardless of its complexity (see, for example, the models of moving boundary problems in heat transfer or elastostatic problems, [Alhama and González Fernández (2002)] and [Morales et al. (2012)], respectively).

After a detailed explanation of the network model design and of how the boundary conditions are implemented, the simulation is carried out in PSpice [Microsim Corporation (1994)], providing the transient perturbation at any point in the output ambience of the code. The widespread use of PSpice and its new versions confirms the applicability of the program to a large variety of circuit simulation problems. It also provides a valuable base of experience that demonstrates the advantages of the powerful, efficient and reliable numerical algorithms that are implemented therein.

Instantaneous pictures of the perturbation along the domain are depicted by processing the output data with MATLAB which, in turn, is also used as programming tool to generate the text file of the network model. To illustrate its application, we first studied a standard case in order to compare the network solutions with those obtained by the explicit finite-difference method, illustrating the deviations between both numerical techniques. In addition, typical 1-D and 2-D scenarios of transversal seismic waves subjected to a Ricker pulse [Ricker (1945)] as excitation and with different types of boundary conditions are also presented.

2 The mathematical model

The governing (hyperbolic) equation for the SH waves in a elastic domain is [Aki and Richards (2002)]

$$\rho\left(\partial^2 v/\partial t^2\right) = \mu\left\{\left(\partial^2 v/\partial x^2\right) + \left(\partial^2 v/\partial z^2\right)\right\} \tag{1}$$

where $v = v\,(x,z,t)$ is the perturbation (transversal displacement), which propagates in all directions of the plane XOZ, and μ and ρ are the transversal elasticity modulus (one of the Lamé parameters) and the density. The ratio $(\mu/\rho)^{1/2} = \beta$ is a positive constant equal to the group velocity of the wave. The stresses related to the displacement v are given by $\sigma_{xy} = \mu\,(\partial v/\partial x)$ and $\sigma_{yz} = \mu\,(\partial v/\partial y)$.

For the excitation point source, the classical Ricker pulse wave is considered, the instantaneous amplitude of which is given by the expression

$$A\,(t) = \left(a^2 - \frac{1}{2}\right) e^{-a^2} \tag{2}$$

with $a = \pi\,(t - t_s)\,/t_p$. Fig. 1 shows the form of this wave as well as its Fourier spectrum for the values t_s=2 s, t_p=1 s. The pulse contains a continuous window of frequencies that extends from 0 to approximately 3 Hz (Fig. 2). Two types of boundary conditions are assumed: homogeneous (Dirichlet), which implies null displacement at the boundary, and the second type (Neumann), which implies free surface or absorbent boundary reflecting continuity in the model.

3 The network model

The first step in the application of the network method, whose purpose is to convert the SH problem into a network (circuit) problem, to design a model for a volume element or cell, whose circuit equations are formally equivalent to the finite-difference differential equations that come from the spatial discretization of the governing (partial differential) equations. Time remains as a continuous variable

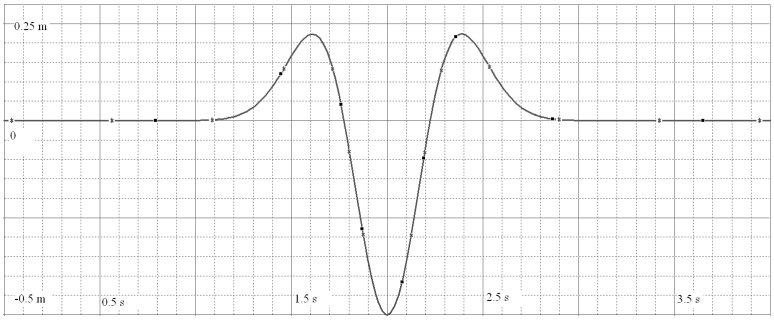

Figure 1: The Ricker pulse, temporal dependence of the amplitude

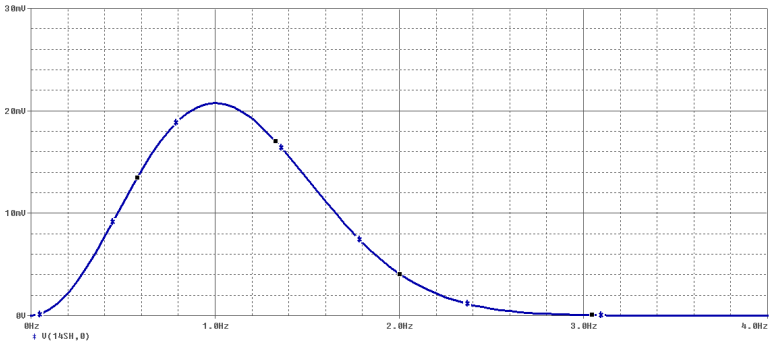

Figure 2: The Ricker pulse, Fourier spectrum

in the network (as in line methods). Once the network cell is designed, the whole model is formed by simple (electrical) ideal connections between adjoining nodes and adding the boundary conditions using suitable electrical components.

Since the simulation code provides the exact solution of the network, errors in the results can only be due to the grid size. The experience gained with the large variety of non-linear problems to which the method has been applied, demonstrates that in 2-D benchmark type problems, a model containing in the order of 50×50 cells provides errors well below 1%. The main advantage of the method is that no mathematical manipulations are required by the user since this work is carried out by the simulation code.

In the network analogy used the following equivalence between the real and electric variables applies at any point of the domain: the displacement or perturbation is related to the electric voltage. Now, the network model of the cell it designed following these steps: i) write the finite-difference differential equation resulting from the spatial discretization of the governing Eq. 1, ii) implement each addend

of the equation as the current of a suitable source whose voltage-current expression is given by a constitutive equation of the same form as that of the addend, iii) balance these currents (as many currents as are addends in the equation) at a common node by simple electrical connection of the components according to the topology (sign of the addend) in the equation, iv) complete the network of the domain by direct electrical connection between adjacent volume elements, v) implement the boundary conditions by suitable electrical devices, and vi) define the sources that implement the excitation or initial conditions.

As is immediately clear, step ii) is easily addressed if the current that defines the source is a linear function of the dependent variable. In this case, the implementation can be done by using simple electrical components such as resistors, for which the relation between current and voltage is algebraic and direct, or capacitors and coils, for which the variables are related by time derivative expressions. However, if the current is not a linear function of the dependent variable –as occurs when the addend that expresses a derivative term is of an order greater than unity or when it is a coupled term containing more than one dependent variable– the implementation requires special attention. In the first case (derivative terms), auxiliary circuits are required to define successive derivatives, while in the second case (coupled terms), the current is implemented by a controlled source whose output can be specified by software as an arbitrary function of the dependent variables defined at any point of the medium.

In order to satisfy the topology of the governing equation, the electrical components related to each term must be suitably placed in the model so that the balance implicit in the equation is satisfied. If this is done, the whole network model is simply equivalent to the problem defined by the governing and boundary conditions equations and, as a consequence, the SH problem is implemented as a circuit problem. A more detailed explanation of the implementation of different types of addends in strongly non-linear and coupled problems can be found in [González Fernández (2002)].

Let us apply the above steps to our problem. Using the nomenclature of Fig. 3 for a symmetric volume element in the domain, the finite-difference differential equation derived from the wave Eq. 1 is

$$\frac{\partial^2 v}{\partial t^2}=\beta^2\left\{\left(\left[\frac{v_{i+\frac{\Delta x}{2}}-v_i}{\frac{\Delta x}{2}}\right]-\left[\frac{v_i-v_{i-\frac{\Delta x}{2}}}{\frac{\Delta x}{2}}\right]\right)\frac{1}{\Delta x}+\left(\left[\frac{v_{i+\frac{\Delta z}{2}}-v_i}{\frac{\Delta z}{2}}\right]-\left[\frac{v_i-v_{i-\frac{\Delta z}{2}}}{\frac{\Delta z}{2}}\right]\right)\frac{1}{\Delta z}\right\} \tag{3}$$

This equation contains five linear terms, four spatially discretized in the right-hand part of the equation plus one on the left, the time second derivative term. First,

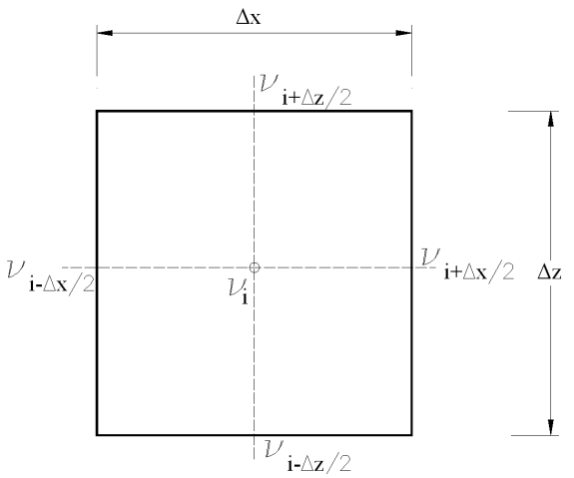

Figure 3: Nomenclature of the volume element or cell

each discretized term is implemented by a resistor (R) since the current of this component (i_R) is related with the voltage by the linear Ohm's law, $i_R = \Delta V/R$. In this way, the values of the resistors are easily obtained using Ohm's law, by considering the term as an electric current:

$$R_{input,x} = \frac{v_i - v_{i-\frac{\Delta x}{2}}}{\beta^2\left[\left(v_i - v_{i-\frac{\Delta x}{2}}\right)\Big/\left(\Delta x/2\right)\right]\Big/\Delta x} = \frac{(\Delta x)^2}{(2\beta^2)} \tag{4}$$

$$R_{input,z} = \frac{v_i - v_{i-\frac{\Delta z}{2}}}{\beta^2\left[\left(v_i - v_{i-\frac{\Delta z}{2}}\right)\Big/\left(\Delta z/2\right)\right]\Big/\Delta z} = \frac{(\Delta z)^2}{(2\beta^2)} \tag{5}$$

$R_{output,x}$ and $R_{output,z}$ are also defined by Eqs. 4 and 5, respectively, due to the symmetry of the cell. To satisfy the topology of Eq. 3, the four resistors are connected between the common (central) node of the cell and their respective boundary nodes, as shown in Fig. 4. Note that we considered the solution $v = v(t)$ at any node of the cell as the voltage in that node.

The term $(\partial^2 v/\partial t^2)$ is also considered as an electric current that counterbalances the other terms and is implemented in a more complex form by auxiliary circuits as follows. The first derivative of the perturbation is obtained by the components E_a, C_a and the null battery $V_{null,a}$. E_a is a (controlled) voltage-source whose input (v_i) is the voltage at the common node of the volume element in the main circuit; its output, also v_i, is applied to the capacitor of capacitance 1.0 farad. In this way,

the current through it is given by $I_C = dv_i/dt$, the first time derivative of the perturbation. This current crosses the battery, which acts as an ammeter (a requirement imposed by PSpice to read the current through the capacitor). The new auxiliary circuit formed by F_a and L_a force the current I_{Ca} to cross through a coil of inductance unity. F_a is a current-source controlled by the current of the battery (I_{Ca}), whose output current is just I_{Ca}. In this way, the voltage through the coil, given by

$$V_{La} = L_a \left(dI_{La}/dt\right) = L_a \left(dI_{Ca}/dt\right) = \left(d^2 v_i/dt^2\right) \tag{6}$$

is the second derivative of the perturbation. Since this is the current that has to be balanced in equation (3), a new dependent current-source connected at the common node of the volume element –whose output current (and input voltage) is the voltage through the coil, $(d^2 v_i/dt^2)$– satisfies this requirement and the five terms of the equation are suitability balanced according to its topology. The complete network model of the volume element is shown in Fig. 4.

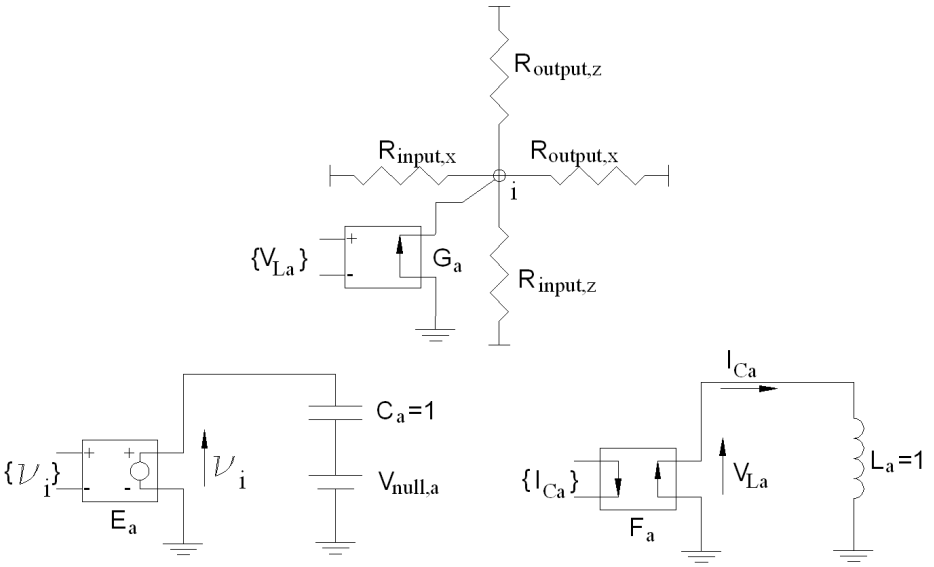

Figure 4: Network model of spatially discretized wave equation

The connection of $N_x \times N_z$ networks, such as that of Figure 4, by ideal electrical contacts covers the physical domain of the problem, which is completed by adding the implementation of boundary conditions at those nodes that form the limit of the domain. Null displacement at the boundaries ($v|_b = 0$) is related to a large inertia; electrically, this means a constant zero voltage at the nodes that define the

contour (Dirichlet homogeneous condition), Fig. 5a. On the contrary, small inertia masses or a free surface, which means free tractions on the boundary surface ($t_y|_b$ = 0), allow the voltage to change in the contour nodes according to the arrival of the perturbation (homogeneous Neumann condition); so, a resistor of very high value (theoretically infinite) is the suitable component to implement this condition, Fig. 5b. This is justified by the connection between traction forces and stress and displacement

$$t_y|_b = \sigma_{xy}\cos\alpha + \sigma_{yz}\cos\gamma = \mu\left(\partial v/\partial x\right)\cos\alpha + \mu\left(\partial v/\partial z\right)\cos\gamma \tag{7}$$

with α and γ being the angles of the outer normal vector to the free surface. When $t_y|_b$ = 0 the value of $\partial v/\partial x = \partial v/\partial z$ = 0, a condition that is only satisfied by a resistor of infinite value. Other more real conditions that partially or totally absorb the energy transported by the wave can be assumed by programming controlled sources.

Finally, in order to release the domain to the excitation source, an electrical switch is required between the Ricker pulse generator and the node where this is applied; the network for this condition is shown in Fig. 5c. The switch opens when the pulse is finished, releasing the node to allow it to move freely.

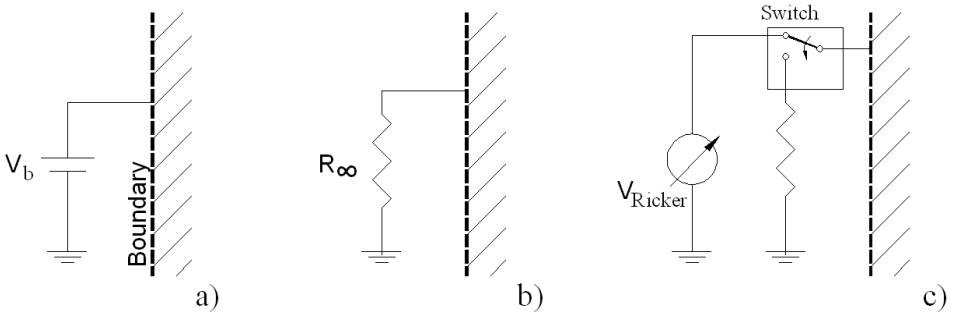

Figure 5: Boundary conditions: a) Dirichlet type, b) Neumann type, c) Switch for the application of a Ricker pulse

Since very few components are required in most cases, including boundary conditions, very few rules are required for the design of the complete model, which is run, without other mathematical manipulations, in a suitable code such as PSpice. Since they work with signals of very high frequencies, the powerful computational algorithms implemented in such codes mean that the simulation reproduces the exact solution of the network model; consequently, the errors can only be attributed to the choice of the grid size. In linear problems such as transversal elastic waves, relative errors are within the permissible ranges in this engineering field.

4 Simulation results

First, the method is applied to solve a kind of benchmark problem in order to compare the results and estimated errors with the solution given by Luzón et. al [2003] using explicit finite-difference methods. The 2-D domain is a square of side 10 m, with free boundaries; the wave velocity is β = 3.5m/s and a Ricker pulse, defined by $t_s = t_p = 2$s, is applied at the center of the domain. A simulation time of 4 s has been considered.

Ten points per wavelength are chosen in order to ensure the quality of the finite-difference solution; for the maximum frequency of the Ricker spectrum (3 Hz), this assumption leads to $\Delta x_{max} = \Delta y_{max} = \beta_{max}/(10 \cdot f_{max}) = 0.2333$m. To fit the grid to 45x45 and 121x121 volume elements, the final values of Δx (and Δy) are 0.2273 and 0.08333 m, respectively. In addition, according to the stability criterion of von Neumann, the maximum time step for the finite-difference solution must satisfy the expression $\Delta t = 2^{-1/2} * \Delta x/\beta_{max}$; we have chosen 0.0066 s (or 600 time intervals), a value that fits the former expression for the two simulations.

Figures 6 and 7 compare network method and finite-difference solutions at two typical points of the domain located in the symmetry line, (5, 6.14) and (5, 7.73), respectively. While both solutions approximately converge when the number of the volume elements is increased, significant deviations appear for small grids. Table 1 shows vertical displacements at selected times (points related to maximum and minimum vertical displacements as well as inflexion points) for both methods with grids of 45×45 and 121×121. For the small grid, standard deviations are also pointed out in the table (taking 50 regular time intervals along the range 0÷4 s) using as approximately exact solutions those of the larger grid.

Table 1: Vertical displacement at typical times and standard deviation

x = 5.00, z = 6.14 m								
Time	1.2	1.6	1.9	2.4	2.8	3.5	4.0	σ
DF 45x45	0.038	0.080	0.012	0.161	0.026	0.080	0.068	0.015
DF 121x121	0.031	0.069	0.014	0.136	0.029	0.059	0.070	0.0026
NSM 45x45	0.029	0.072	0.031	0.149	0.051	0.070	0.070	0.0096
NSM 121x121	0.030	0.067	0.018	0.133	0.032	0.058	0.069	-
x = 5.00, z = 7.73 m								
Time	1.8	2.1	2.3	2.8	3.2	3.6	4.0	σ
DF 45x45	0.039	0.054	0.030	0.091	0.002	0.047	0.017	0.0066
DF 121x121	0.032	0.046	0.023	0.079	0.009	0.047	0.013	0.0016
NSM 45x45	0.033	0.051	0.013	0.083	0.023	0.050	0.009	0.0053
NSM 121x121	0.031	0.046	0.019	0.076	0.011	0.045	0.012	-

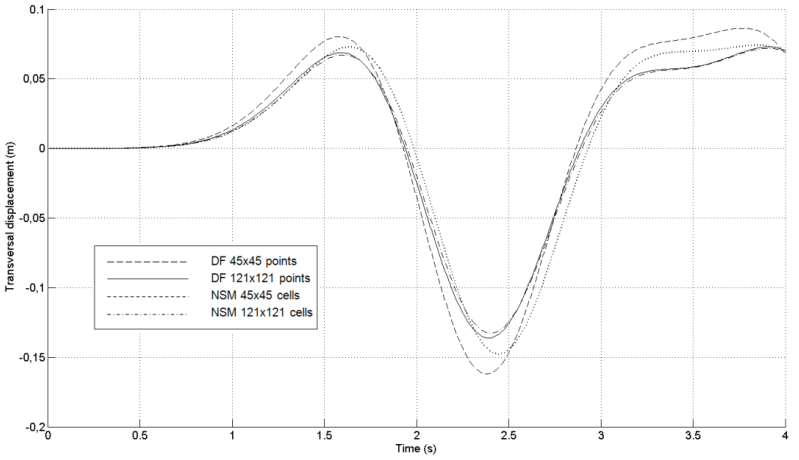

Figure 6: Perturbations at $x = 5$, $z = 6.14$ m

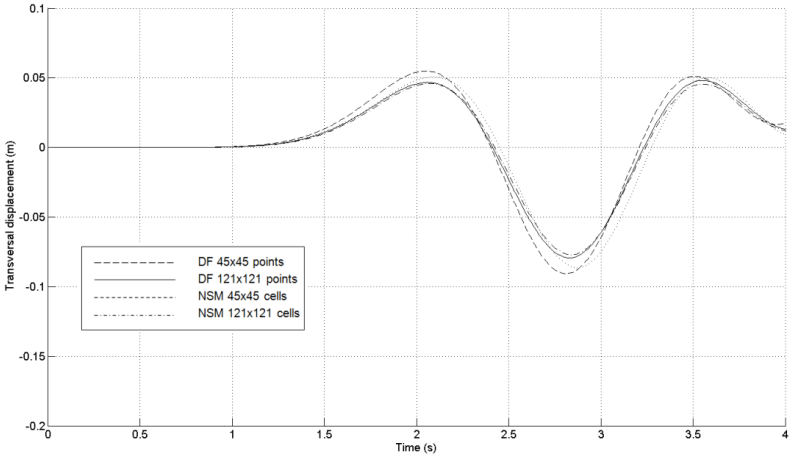

Figure 7: Perturbations at $x = 5$, $z = 6.14$ m

Secondly, two new illustrative applications of the model to 1-D and 2-D domains are studied. For the 1-D case, the following values are imposed: ρ = 3,000 kg/m^3; μ = 4·10^9 N/m^2, L (length of the domain) = 5,000 m (resulting in propagation velocity of β = 1,155 m/s), time window of the simulation 0-20 s and N (number of volume elements in the domain) = 191. To simulate the absorbent condition at the ends of the domain, 10 new volume elements of a length 10 times larger than that of the domain have been added (5 on the right of the domain and 5 on the left). Ricker's condition for t_s=2 s, t_p=1 s (Fig. 5c) is applied to the central node of the volume element 101, so that complete symmetry is imposed on the problem.

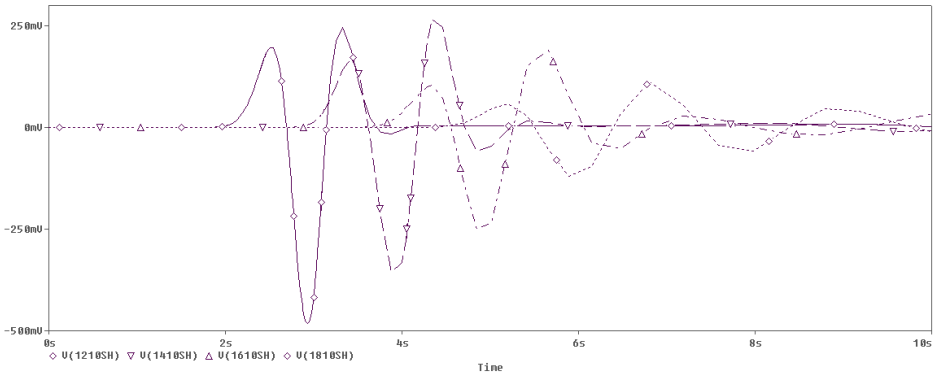

Figure 8: Instantaneous perturbation at four typical locations, x = 3000, 3500, 4000 and 4500 m

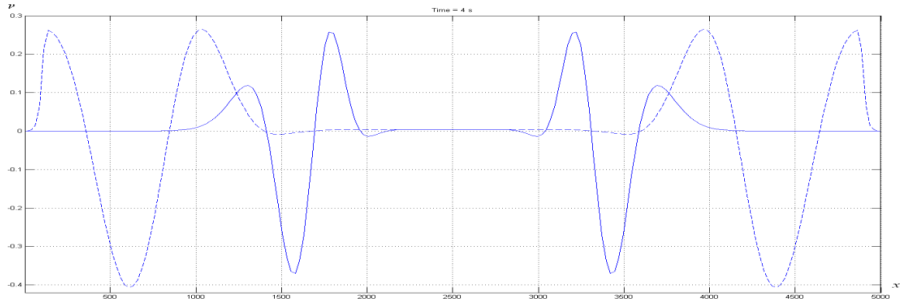

Figure 9: Domain perturbation at t = 4 s. Continuous line: β = 1155, dashed line: β = 2309 m/s

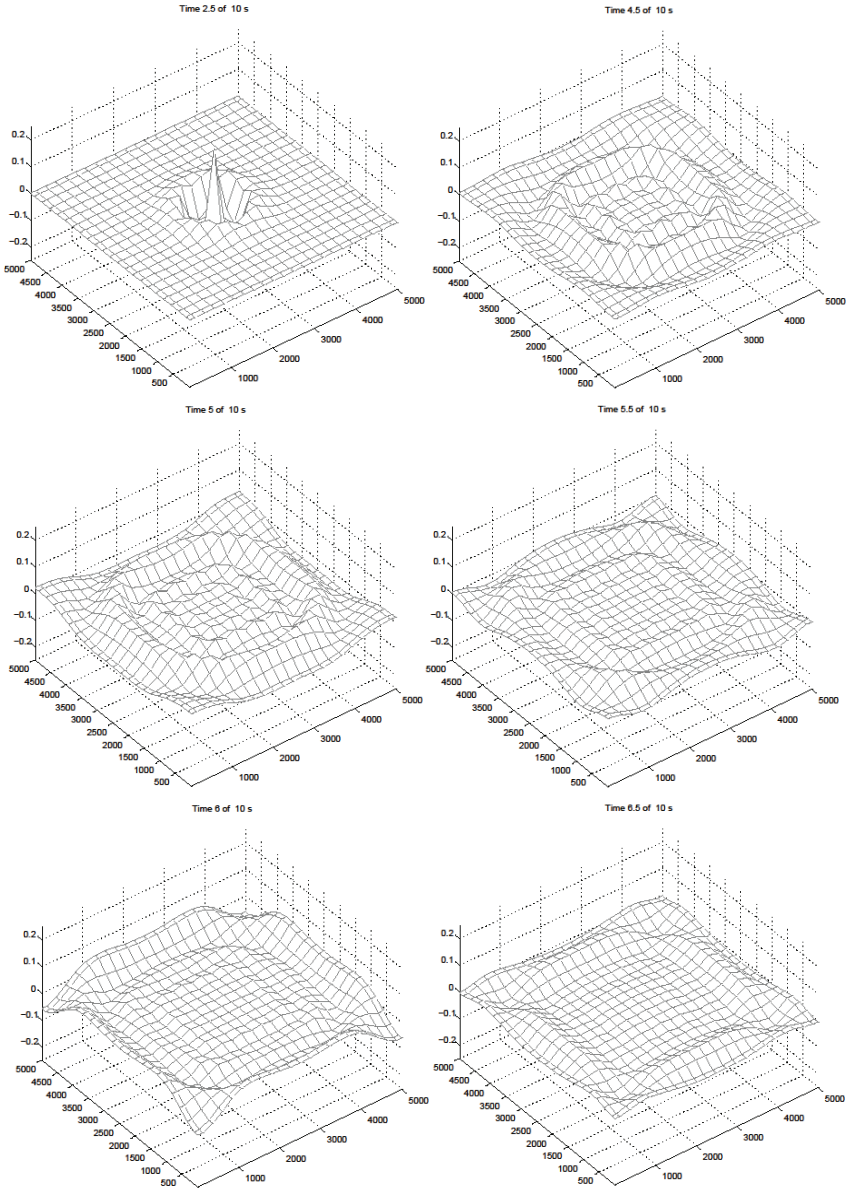

Figure 10: Domain perturbation at t = 2.5, 4.5, 5.0, 5.5, 6.0 and 6.5 s. Excitation located at the centre of the domain

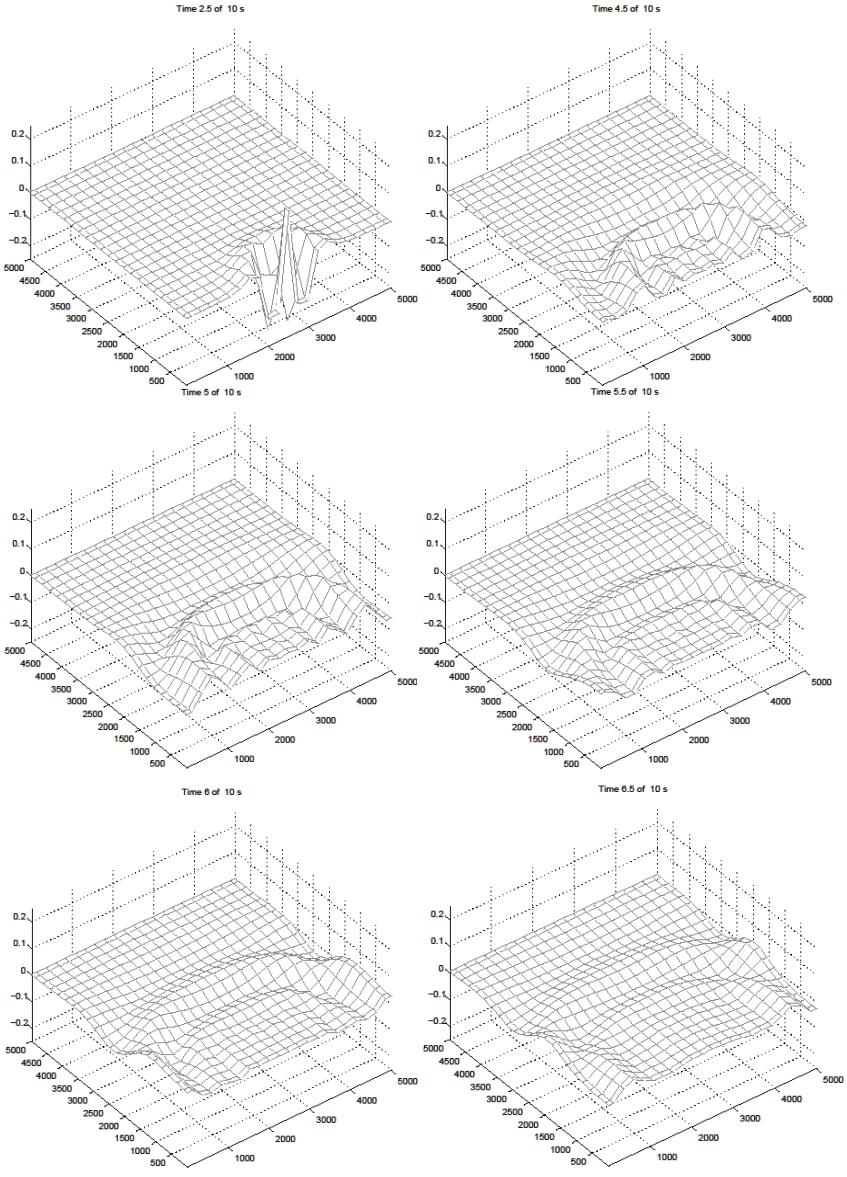

Figure 11: Domain perturbation at t = 2.5, 4.5, 5.0, 5.5, 6.0 and 6.5 s. Excitation located at the centre of a side

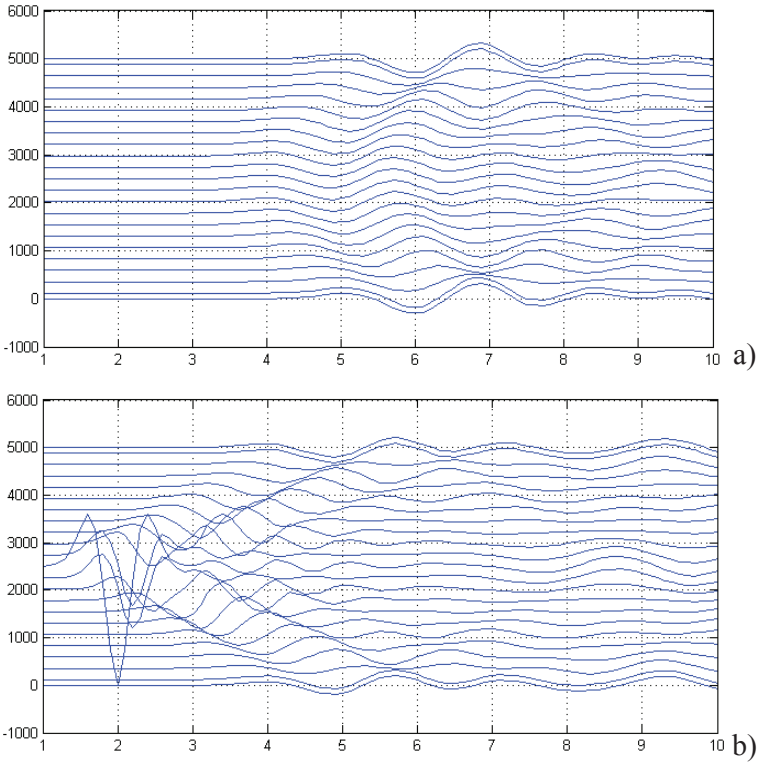

Figure 12: Transient perturbation along the lines: a) $x = 0$ and b) $x = 2{,}500$ m

The simulation provides the results shown at Figs. 8 and 9. In the first, the instantaneous perturbation for four typical locations of the domain is depicted in the PSpice ambience. As time progresses the perturbation reaches points far from the source and dispersion phenomena are clearly appreciated as a result of wave deformation. The deformed domain at t = 4 s, in the MATLAB ambience, for two values of the wave velocity (β = 1,155 and 2,309 m/s) are represented in Figure 7, showing, once again, the dispersion effect. The computational time for this application is 96 s in an AMD ATHLON 64×2 Dual Core Processor 5200+, 1.80 GHz PC.

As regards the 2-D application, the following parameters have been chosen: $\rho = 10^3$ kg/m^3, $\beta = 10^3$ m/s, the domain extends to the square $L_x = L_z$ = 5,,000 m, the mesh is formed by 21×21 volume elements and the time window is reduced to 0-10 s. Ricker pulses under the condition given by Fig. 5c, with t_s=2 s, t_p=1 s, are successively applied to the central node of the volume element (11,11) and

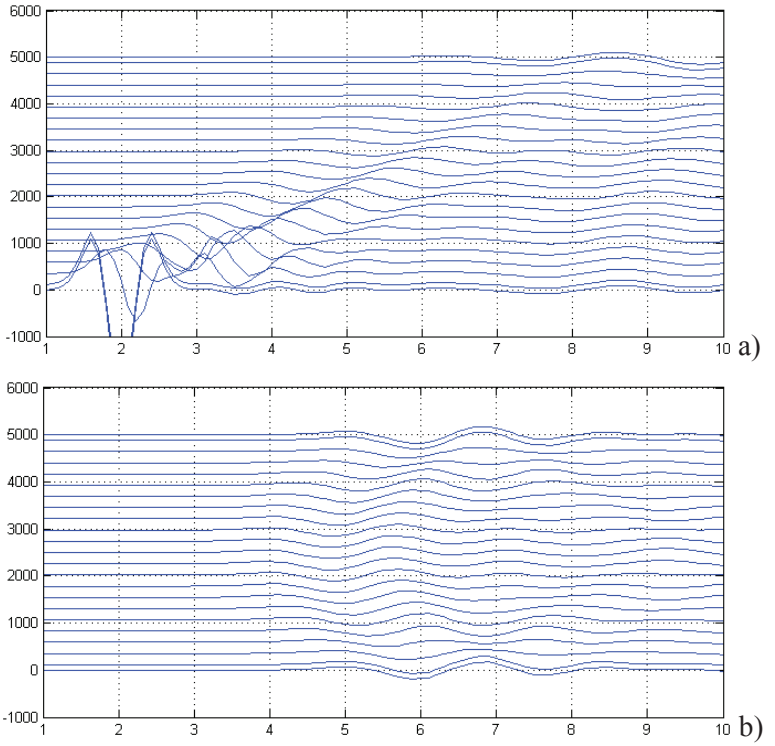

Figure 13: Transient perturbation along the lines: a) x = 2,500 and b) z = 2,500 m

to the centre of a boundary side (1,11). The boundary condition is changed to a Neumann type condition (free boundary), equivalent to assuming null shear stress, in the form

$\sigma_{xy} = \mu\left(\partial v/\partial x\right)$, at x=0 and $x = L_x$; $\sigma_{yz} = \mu\left(\partial v/\partial z\right)$, at z=0 and $z = L_z$(8)

Figs. 10 and 11 show the domain perturbation at successive times (the first picture of both figures corresponds to a time for which the Ricker pulse has not finished). As the time increases a smoother representations emerges due to dispersion phenomena. Finally, Figs. 12 and 12 show typical representations of the seismic wave propagation corresponding to instantaneous perturbation at two typical sections with the excitation applied at the center of the domain and at the center of the boundary side, respectively; these displacements are shown using a scale of 5,000. The computational time for this application is 1,220 s.

5 Conclusions

The network method demonstrated to be an efficient tool for solving the transversal wave equation problem by numerical simulation. The design of the network, as well as the implementation of the boundary conditions, in all cases, are relatively direct and easy, since very few rules are required for the design thanks to the existence of the special controlled sources defined in the libraries of the circuit simulation codes. In addition, no mathematical manipulation other than the spatial discretization of the partial differential equation is required since this work is done by the software PSpice and the data treatment routines. For a standard problem, simulation results can be considered to suitably match those obtained with the explicit finite-difference method.

References

Akbari, A.; Bagri, R.; Bordas, S. P. A.; Rabczuk, T. (2010): Analysis of thermoelastic waves in a two-dimensional functionally graded materials domain by the Meshless Local Petrov Galerkin (MLPG) method. *CMES-Computer Modeling in Engineering and Sciences,* vol. 65, no. 1, pp. 27-74.

Aki, K.; Richards, P. G. (2002): *Quantitative Seismology, Second Edition.* University Science Books, Sausalito, California.

Alhama, I.; Alhama, F.; Soto Meca, A. (2012): The network method for a fast and reliable solution of ordinary differential equations: Applications to non-linear oscillators. *Comput. Electr. Eng.*, vol. 38, no. 6, pp. 1524–1533.

Alhama, F.; González Fernández, C. F. (2002): Network simulation method for solving phase change heat transfer problems with variable thermal properties. *Heat and Mass Transfer*, vol. 38, pp. 327-335.

González Fernández, C. F. (2002): *Network Simulation Method.* Ed. J. Horno, Research Signpost. Trivandrum-695023, India.

Incropera, F. P.; De Witt, D. P. (1996): *Fundamentals of heat and mass transfer.* John Wiley & Sons, New York.

Luzón, F.; Ramírez, L.; Sánchez-Sesma, F. J.; posadas, A. (2003): Propagation of SH elastic waves in deep sedimentary basins with an oblique velocity gradient. *Wave motion*, vol. 38, pp. 11-23.

Martin-Vaquero, J; Vigo-Aguiar, J. (2006): Exponential fitting BDF algorithms: Explicit and implicit 0-stable methods. *Journal of computational and applied mathematics*, vol. 192 (1), pp. 100-113.

Microsim Corporation (1994): PSICE, Release 6.0. Microsim Corporation, 20 Fairbanks, Irvine, California 92718.

Mills, A. F. (1995): *Heat and Mass transfer.* Richard D. Irwin, Inc. Chicago.

Morales, J. L.; Moreno, J. A.; Alhama, F. (2011): Numerical solutions of 2-D linear elastostatic problems by network method. *CMES-Comp. Model. Eng. Sci.,* vol. 76, no. 1, pp.1-18.

Morales, J. L.; Moreno, J. A.; Alhama, F. (2012): New additional conditions for the numerical uniqueness of the Boussinesq and Timpe solutions of elasticity problems. *Int. J. of Computer Mathematics*, vol. 89, no. 13-14, pp. 1794-1807.

Moreno, J. A.; Gómez De León Hyjes, F. C.; Alhama, F. (2007): Solution of temperature fields in hydrodynamics bearing by the numerical network model. *Tribol. Int.*, vol. 40, pp. 139-145.

Natesan, S; Vigo-Aguiar, J; Ramanujam, N. (2003): A numerical algorithm for singular perturbation problems exhibiting weak boundary layers. *Computers & mathematics with applications*, vol. 45, no. 1-3, pp. 469-479.

Ricker, N. (1945): The computation of output disturbances from amplifiers for true wavelet inputs. *Geophysics,* vol. 10, pp.207-220.

Simos, T. E.; Vigo-Aguiar, J. (2003): A dissipative exponentially-fitted method for the numerical solution of the Schrödinger equation and related problems. *Comput. Phys. Commun.*, vol. 152, no. 3, pp. 274-294.

Soto Meca, A.; Alhama, F.; González-Fernández, C. F. (2007): An efficient model for solving density driven groundwater flow problems based on the network simulation method. *J. Hidrology*, vol. 339, pp. 39-53.

Vigo-Aguiar, J.; Natesan, S. (2006): An efficient numerical method for singular perturbation problems. *J. Comput. Appl. Math.*, vol. 192, no. 2, pp. 132-141.

Zhuang, X.; Augarde, C.; Bordas, S. (2011). Accurate fracture modelling using meshless methods and level sets: formulation and 2D modelling. *International Journal for Numerical Methods in Engineering*, vol. 86, pp. 249-268.

Zhuang, X.; Augarde, C.; Mathisen, K. (2012): Fracture modelling using meshless methods and level sets in 3D: framework and modelling. *International Journal for Numerical Methods in Engineering*, vol. 92, pp. 969-998.